

See discussions, stats, and author profiles for this publication at: <https://www.researchgate.net/publication/282803541>

A Nonlinear Frame Test Structure with Repeatable Behavior for Experimental Dynamic Response History Investigation

Article in *Journal of Earthquake Engineering* · July 2015

DOI: 10.1080/13632469.2015.1046571

CITATION

1

READS

204

4 authors, including:



Andrew Paul O'Donnell

AIR Worldwide

9 PUBLICATIONS 44 CITATIONS

SEE PROFILE



Yahya C. Kurama

University of Notre Dame

138 PUBLICATIONS 4,146 CITATIONS

SEE PROFILE



Erol Kalkan

QuakeLogic Inc.

177 PUBLICATIONS 3,622 CITATIONS

SEE PROFILE

A Nonlinear Frame Test Structure with Repeatable Behavior for Experimental Dynamic Response History Investigation

A. P. O'DONNELL, Y. C. KURAMA, A. A. TAFLANIDIS,
and E. KALKAN

QUERY SHEET

This page lists questions we have about your paper. The numbers displayed at left can be found in the text of the paper for reference. In addition, please review your paper as a whole for correctness.

- Q1:** Au: Is the shortened title above OK for the running head?
- Q2:** Au: Your FundRef details have been set in your proof. These have been updated from the original manuscript. Please check and confirm they are correct.
- Q3:** Au: Please clarify author names in Dyke *et al.*, [1998] as there are some last names missing.
- Q4:** Au: Are there editor names for Lignos *et al.*, 2011.
- Q5:** Au: Please provide first initials for Nader and Astaneh-Asl, 1996.
- Q6:** Au: Please provide vol., issue, and page numbers for O'Donnell *et al.*, 2012.

TABLE OF CONTENTS LISTING

The table of contents for the journal will list your paper exactly as it appears below:

A Nonlinear Frame Test Structure with Repeatable Behavior for Experimental Dynamic Response History Investigation
A. P. O'Donnell, Y. C. Kurama, A. A. Taflanidis, and E. Kalkan

A Nonlinear Frame Test Structure with Repeatable Behavior for Experimental Dynamic Response History Investigation

A. P. O'DONNELL¹, Y. C. KURAMA¹, A. A. TAFLANIDIS¹,
and E. KALKAN²

¹Civil and Environmental Engineering and Earth Sciences, University of Notre Dame, Notre Dame, Indiana, USA

²Earthquake Science Center, United States Geological Survey, Menlo Park, California

This article describes a novel, small-scale nonlinear beam-column connection and an associated six-story frame test structure for the experimental dynamic response investigation of multi-story buildings subjected to earthquake loading. The objective is to create a re-configurable, reusable experimental platform on which several aspects of nonlinear dynamic response can be investigated through successive, exhaustive testing under suites of earthquake records. Static and dynamic calibration tests demonstrate excellent test-to-test repeatability of four structure configurations. These results confirm that the properties of each configuration (period, strength, energy dissipation) remain invariant, thus allowing future experimental investigations (e.g., of peak engineering demands) under earthquake loading.

Keywords Nonlinear Beam-Column Connection; Nonlinear Frame; Nonlinear Response History; Shake Table Testing; Dynamic Testing Repeatability

1. Introduction

The seismic analysis/design of most civil engineering structures is based on significant nonlinear behavior under large earthquake loading [Ibarra *et al.*, 2005; Goulet *et al.*, 2007; Elnashai and Di Sarnio 2008; Erberik *et al.*, 2012; Seo and Sause, 2013]. The motivation for the nonlinear beam-column connection and the associated multi-story frame structure described in this article is the development and calibration of a reusable, re-configurable experimental platform that can be used in future studies to investigate the seismic demands (e.g., peak lateral displacements) of building frame structures under earthquake loading. Most of the previous experimental research on the nonlinear dynamic response of building structures under earthquake loading has focused on large-scale specimens [Schoettler *et al.*, 2009; Panagiotou *et al.*, 2011; Kim *et al.*, 2012; Stavridis *et al.*, 2012]. A major limitation of these studies is that only a few specimens could be tested and under only a small number of ground motion records (e.g., Nader and Astaneh-Asl, 1996; Filiatrault *et al.*, 2002, among others) due to the small number of large-scale shake-table facilities in the U.S. and abroad and the costs associated with these experiments. While a much larger database of shake-table experiments is available for small-scale specimens, many of these studies were

Received 24 January 2014; accepted 27 April 2015.

Address correspondence to A. A. Taflanidis, Civil and Environmental Engineering and Earth Sciences, University of Notre Dame, 156 Fitzpatrick Hall, Notre Dame, IN 46556. E-mail: a.taflanidis@nd.edu

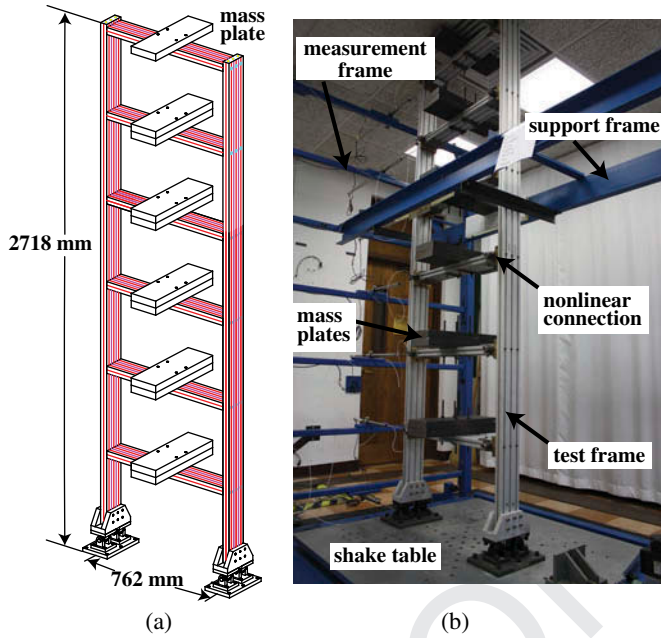


FIGURE 1 Six-story frame: (a) schematic (beam-column connections not shown); (b) test setup.

limited to elastic response (e.g., Dyke *et al.*, 1998; Mo and Lee, 2000; Lafortune *et al.*, 2007; O'Donnell *et al.*, 2012) and the studies that did investigate nonlinear response (e.g., Rodgers and Mahin 2003; Rodriguez *et al.*, 2007; Lignos *et al.*, 2011] were limited to structures with damaged components that had to be replaced (i.e., the nonlinear test specimens were not truly re-usable). As such, the number of tests that could be conducted was small, resulting in limited tests to demonstrate the repeatability of each structure. To the best of the authors' knowledge, the test bed described in this paper provides an enhanced repeatability over similar structures that have been developed previously, and has also been subjected to a more rigorous assessment of its repeatability.

As shown in Fig. 1, the experimental platform described in this paper utilizes a reusable, six-story, single-bay test frame constructed from extruded aluminum beam and column members. The frame dimensions, which were determined based on the size limitations of the shake table, correspond to a building length-scale of, approximately, $S_L = 1/10$ and a time scale of $S_T = 1/3$. More information on the general features of the frame can be found in O'Donnell *et al.* [2012]. One of the key features of the structure is a reusable nonlinear beam-column connection design that can consistently emulate the behavior of representative structural connections under earthquake loading. While the beam and column members of the test specimen are designed to remain linear elastic, the nonlinearity and energy dissipation during an earthquake are concentrated at the beam-column connections. The lateral strength of the structure can be altered by prescribing the moment strength for the beam-column connections. The fundamental period of vibration can be varied by changing the amount of mass (i.e., the number of mass plates) attached to the floor and roof levels.

Since the primary intended use of the experimental platform is to conduct a large number of shake table tests using each structural configuration (with a prescribed lateral

strength and fundamental period), an important requirement is that the behavior of the frame specimen be repeatable such that each test starts from the same initial conditions with the structure possessing the same structural properties from test to test. In other words, while the behavior of the structure is allowed to go into the nonlinear range during each ground motion, the initial properties (i.e., lateral stiffness, period, damping) should remain invariant between the tests. In accordance with this requirement, this article focuses on the design and calibration of the nonlinear connection as well as the repeatability of the multi-story frame test specimen, especially when considering the median engineering demand parameters (e.g., peak displacements) from a suite of records.

2. Beam-Column Connection

The development of the beam-column connection requires a reusable, damage-free component that can satisfy the functional demands associated with nonlinearity, reconfigurability, and repeatability without any permanent change in the behavior of the structure from test to test. The connection needs to act in a linear-elastic manner up to a prescribed “yield” moment, after which the behavior becomes nonlinear to emulate representative structural connections during strong earthquake loading. The initial stiffness, prescribed yield moment, post-yield behavior, and hysteretic characteristics of the connection need to remain consistent under repeated use, while the yield moment can be calibrated to result in a desired lateral strength and behavior for the multi-story frame.

The design of the connection was based on a rotational friction damper that was previously developed for supplemental energy dissipation in seismic precast concrete frame structures [Morgen and Kurama, 2008]. Precast concrete beam-column subassembly tests under quasi-static loading as well as isolated damper experiments under dynamic loading were conducted [Morgen and Kurama, 2009] with two types of friction interfaces: (1) lead-bronze (brass) alloy against stainless steel and (2) lead-bronze alloy against cast steel alloy. The use of lead-bronze alloy at the friction interfaces is desirable because the material “self-lubricates” when rubbing against an adjacent metal surface, which helps to reduce the phenomenon of stick-slip and results in a consistent value for the coefficient of friction. Sample isolated damper test results for lead-bronze alloy against stainless steel friction interfaces can be seen in Fig. 2. The experiments showed that friction dampers can provide: (1) repeatable, damage-free behavior that is largely independent of slip velocity and displacement amplitude (a desirable characteristic for design and performance); (2) close-to-rectangular force-displacement characteristics with consistent strength and large energy dissipation per cycle; and (3) large initial stiffness allowing slip to occur early in the response, providing energy dissipation beginning at small lateral displacements of the structure. The results were used to determine the static and kinetic coefficients of friction, μ_{static} and $\mu_{kinetic}$, respectively, and the effect of the normal force, F_n acting on the friction interfaces.

Based on the results from Morgen and Kurama [2008, 2009], a nonlinear beam-column connection utilizing lead-bronze alloy (CDA 932 bearing bronze) against stainless steel (cold drawn 303 annealed stainless steel) friction interfaces was developed for this research. As shown in Fig. 3, the connection component bolted to the beam end is fabricated out of stainless steel and the component bolted to the column is lead-bronze alloy. The moment strength of the connection is controlled by the normal force, F_n applied to the friction interfaces using a high-strength (ASTM A574 alloy steel) machined shoulder bolt. The normal force F_n generates the friction required to develop the moment resistance when the connection components are rotated with respect to one another. Belleville washers are

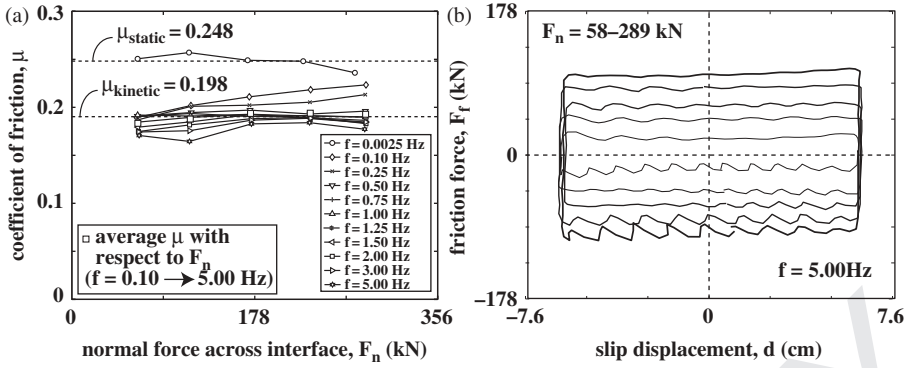


FIGURE 2 Characterization of lead-bronze alloy against stainless steel friction interfaces: (a) coefficient of friction (b) friction force vs. slip displacement (adapted from Morgen and Kurama, 2009).

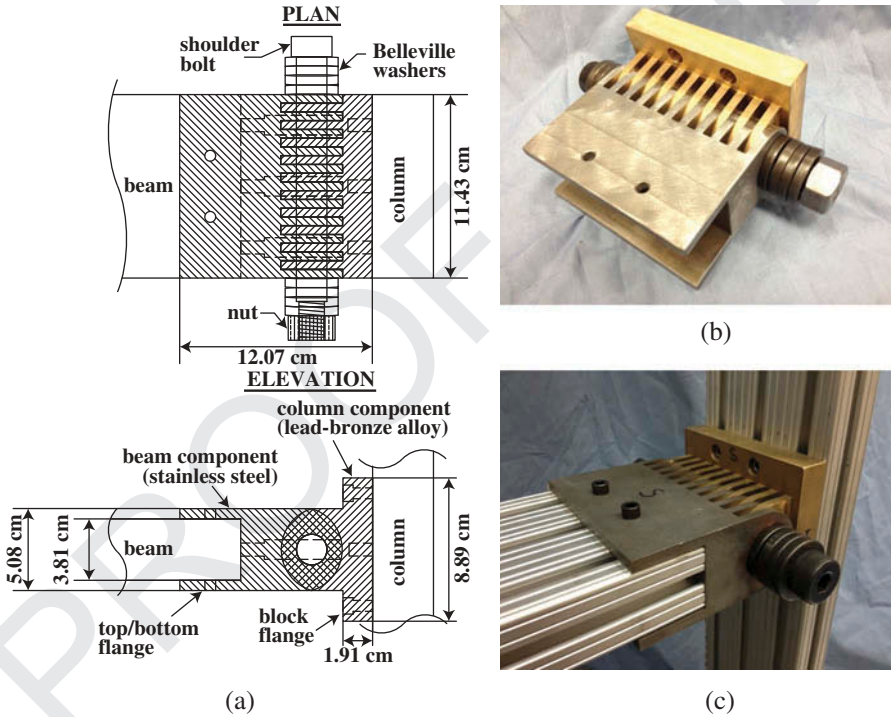


FIGURE 3 Nonlinear connection design: (a) schematic; (b) photograph; and (c) as assembled.

used to maintain a consistent level of normal force during each test due to their spring-like behavior and consistency through many loading and unloading cycles. 110

The outside dimensions of the connection components were selected to be compatible with the 38-mm thickness and 114-mm width of the beam members of the six-story frame. Each “tooth” (on both the lead-bronze and the stainless steel components of a connection) was manufactured to be 5.39-mm thick and each void between two teeth was 5.49-mm thick; thus, leaving an extremely small tolerance gap of 0.05 mm on both sides of each 115

tooth. This design ensured that the number of friction interfaces was adequate (total of 21 teeth and 20 friction interfaces) to achieve the desired moment strength of the connection without overstressing the shoulder bolt or washers, while allowing the teeth to experience a very small amount of elastic deformation to achieve a near-even normal stress distribution across the friction interfaces. Both joint components were manufactured to a very high level of precision using a computer numerical control (CNC) machining process, resulting in a tightly assembled system with a fairly linear direct relationship between the connection strength and the applied torque as shown later in this article. 120

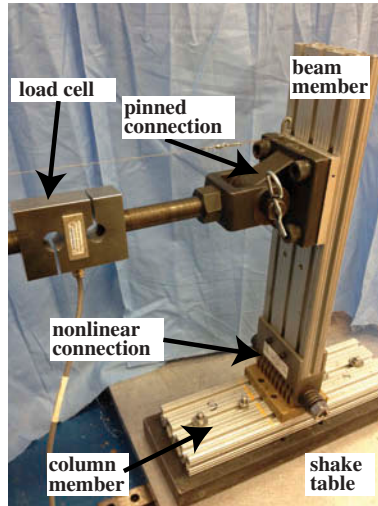
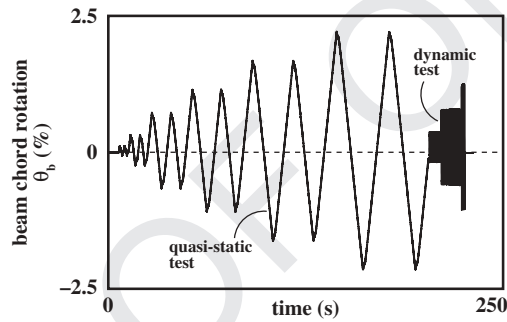
Block flanges were included in the lead-bronze component to allow for attachment bolts to the column, ensuring essentially no slack between the connection and the column. Similarly, top/bottom flanges were included in the stainless steel component to accommodate the placement of attachment bolts to the beam, providing essentially no slack between the connection and the beam. Additional attachment bolts to the beam and column members were placed through the mid-thickness of the connection components. 125

A machined shoulder bolt was used to join the connection components and apply the normal force due to the high precision with which the shoulder diameter is made. It was determined that a 19-mm-diameter bolt would be adequate to achieve the desired connection strength without the need to overstress the bolt during repeated use. High strength, structural-grade Belleville washers with an outer diameter of 34-mm (to bear within the diameter of the teeth rotation zone) and an inner diameter of 20-mm (to fit over the shoulder of the shoulder bolt) with a load rating of 89-kN were used to generate sufficient normal force without yielding. Multiple Belleville washers were used in series to increase the number of nut turns required to reach a given level for force normal to the friction interfaces, F_n and thereby reduce the sensitivity of F_n to the number of turns. The Belleville washers were arranged such that the broader end of their conical profile was bearing against the outside face of the connection to provide a more even compressive stress distribution to the friction interfaces. 130
135
140

3. Connection Behavior and Calibration

The moment capacity of each nonlinear beam-column connection is related to the normal force, F_n applied to the friction interfaces. However, since it was not practical to incorporate a load cell into the design of the connection, the normal force had to be regulated through a means other than direct measurement. Bolt gauges were not used because of increased specimen preparation time from test to test. Direct tension indicators were also deemed impractical since new indicators would have to be installed in the connections after each test. Therefore, an electronic calibrated torque wrench was used to determine the amount of torque applied on the normal bolt and relate the measured torque to the moment strength of the connection. A similar method is often used in the construction of bolted connections in steel structures where tighter torque values are attributed to tighter connections that are often referred to as “slip-critical.” 145
150

Static and dynamic tests of an isolated beam-column subassembly were used to calibrate each connection by correlating its moment strength, M_{cm} to the torque, T_a applied on the shoulder bolt. As shown in Fig. 4, the assembly consisted of a vertically oriented beam member, a column member fixed horizontally to the shake table, and a nonlinear connection between the beam and the column. During each test, the shake table was moved through a reversed-cyclic displacement history at different excitation amplitudes and frequencies. A pin-ended threaded rod with a load cell was connected to the beam at a distance of 375 mm from the column face (which is close to the midspan location of the beams in the six-story structure). The other end of the threaded rod assembly was connected to 160

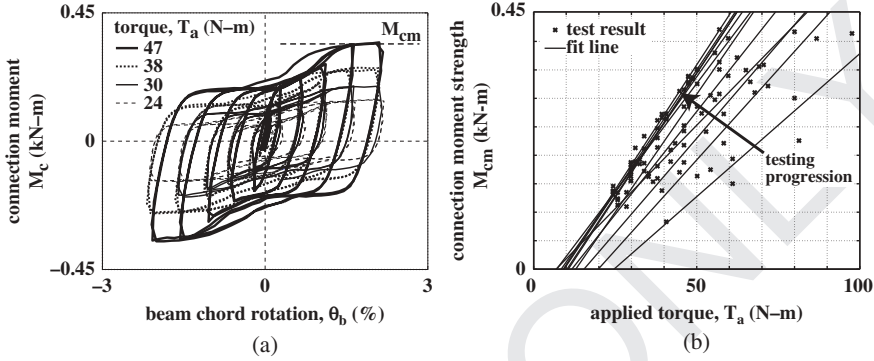
**FIGURE 4** Connection test setup.**FIGURE 5** Combined test history.

a rigid steel reaction frame to keep the beam stationary while measuring the resulting force as the nonlinear connection was rotated through the displacements of the shake table. Displacement transducers mounted to an adjacent wall (isolated from the reaction frame) were used to measure the beam chord rotation, θ_b .

As shown in Fig. 5, each connection subassembly was first subjected to a slow quasi-static test with two displacement cycles at six different amplitudes up to a maximum beam chord rotation of $\theta_b = 2.2\%$, which was determined based on the largest expected connection rotations in the six-story frame. The quasi-static tests were conducted using a constant velocity during the applied loading history. Immediately following the quasi-static loading, each connection was subjected to the dynamic test combinations in Table 1, which were determined from the expected dominant frequencies of the test structures. For each combination of beam chord rotation and excitation frequency in Table 1, the subassembly was subjected to 10 loading cycles, resulting in a dynamic loading sequence of 70 cycles. Similar to other studies on friction dampers [Gregorian *et al.*, 1993; Way 1996; Morgen and Kurama 2009], no significant dependency of the dynamic connection response to the excitation frequency was found. Note that even though higher mode vibrations in a multi-story frame structure can subject the beam-column connections to greater (i.e., higher mode) excitation frequencies than the frequencies listed in Table 1, this effect is considered

TABLE 1 Dynamic connection test parameters

| Beam Chord Rotation (%) | | Excitation Frequency (Hz) | | |
|----------------------------|-----|------------------------------|------|---|
| 0.27 | 2.3 | — | 4.35 | — |
| 0.69 | 2.3 | 3.8 | 4.35 | 5 |
| 1.11 | — | — | 4.35 | — |

**FIGURE 6** Beam-column moment-rotation behavior of Connection 1: (a) hysteresis results and (b) connection moment strength.

insignificant as compared to the variations from the connection normal bolt force (since the bolt force was not directly measured).

Sample quasi-static connection moment, M_c vs. beam chord rotation, θ_b behaviors from the beam-column subassembly tests are shown in Fig. 6a. The connection moment was determined by multiplying the measured load cell force with the distance to the column face (375 mm). As can be seen from Fig. 6a, the connection exhibits a high initial stiffness before beginning to slip and rotate, ultimately reaching a plateau through a pinched hysteretic behavior. The pinched behavior occurs because at zero rotation, the fixed ends of the teeth on the beam and column components of the connection are furthest away from each other, but as the beam and column components are rotated, the fixed ends move closer to each other, thus effectively stiffening the connection. As expected, the connection moment strength increases as the torque, T_a on the shoulder bolt is increased.

The inability to directly measure the connection moment or the normal bolt force introduces variability and uncertainty in the repeatability of the connection strength and behavior. To quantify this variability and calibrate the relationship between the applied clamping torque and the moment strength for each connection, a series of tests were conducted. After each test, the shoulder bolt was fully loosened, the connection was brought back to plumb, and the bolt was re-tightened to the next torque value. To minimize the variability, each connection was tested with the same set of shoulder bolt and Belleville washers, as would be used in the full six-story frame structure.

The applied bolt torque, T_a vs. the resulting connection moment strength, M_{cm} from the calibration tests of a typical connection is shown using the x markers in Fig. 6b. As shown in Fig. 6a, the moment strength, M_{cm} was calculated as the average moment resistance of the connection after the attainment of the ultimate strength plateau during quasi-static

testing. In Fig. 6b, the straight lines represent the best linear fit to the calibration data for each subset of eight tests collected sequentially throughout the testing of a connection. The arrow represents the progression from earlier tests to eventual stability achieved in the later tests of the same connection. Repeated testing showed that each connection initially underwent a period of “stiffening” as it was tested from its virgin, untested state until it eventually stabilized and the relationship between moment strength and applied torque was sufficiently repeatable and predictable. This stiffening was most likely attributable to the removal of loose particulates from the friction interfaces. Each connection was subjected to a minimum of 80 tests until at least 40 tests (5 subsets of 8) were determined to be sufficiently repeatable. The achievement of adequate stability in the performance of each connection was defined as the discontinued increase in the slope of the linear regression defining the torque to moment relationship for the i^{th} subset as compared to subset $i-1$. Some of the connections were able to reach stability within the minimum 80 tests while others required up to 128 tests to exhibit behavior that was deemed stable. Eventually, a stable set of 40 tests was produced for each connection, as shown in Fig. 7, correlating applied bolt torque, T_a to the moment strength, M_{cm} .

As can be seen from the dashed lines in Fig. 7 depicting a band of \pm one standard deviation, σ from the fit line, each connection demonstrated a different level of uncertainty in its performance despite the fact that all 12 connections were fabricated and tested using the same process. Table 2 lists the standard deviation of the measured connection strength from the linear regression line for each connection. Since it is reasonable to expect that the nonlinear connection rotations will be greatest in the lower floors of the six-story frame structure, the connections with lower standard deviation were placed in the lower floors and those with larger standard deviation were placed in the upper floors. This was done in an effort to minimize the variability in the behavior of the overall frame. The ordering of the connection calibration plots in Fig. 7 visually illustrates how the connections were distributed within the frame.

As example of typical results, Fig. 8 shows the quasi-static moment versus rotation (M_c vs. θ_b) behaviors from four stable tests of Connection 1 (with the lowest standard deviation in Table 2) and Connection 4 (with the highest standard deviation in Table 2) with an applied torque of $T_a = 26$ N-m. To result in the largest extent of variability possible, the tests were conducted in a non sequential manner. It can be seen that the hysteretic behavior of Connection 1 demonstrates excellent repeatability. While the increased variability in Connection 4 is noticeable, the behavior is acceptable for use in the upper levels of the six-story frame structure. The effect of the connection variability on the behavior of the six-story frame is investigated in the next section.

4. Six-Story Frame Behavior and Repeatability

This section discusses the behavior and repeatability of the six-story frame structure using the 12 nonlinear beam-column connections. To ensure that the beam-column connections undergo nonlinear rotations as intended in their design, the dynamic behavior of the six-story frame was monitored using three-dimensional digital image correlation (3D-DIC) during a limited number of initial trial tests [McGinnis *et al.*, 2012]. Figure 9 compares the observed deformed shapes of two beams from the lowest two floors of the structure at the instant of maximum inter-story drift during a dynamic base excitation. One of the beams was rigidly connected to the columns while the other beam was fastened to the column using nonlinear friction beam-column connections, as described in Sec. 2. The 3D-DIC measurements show that the beam with nonlinear connections essentially displaced like a rigid body, with most of the rotations concentrated in the connections rather than distributed

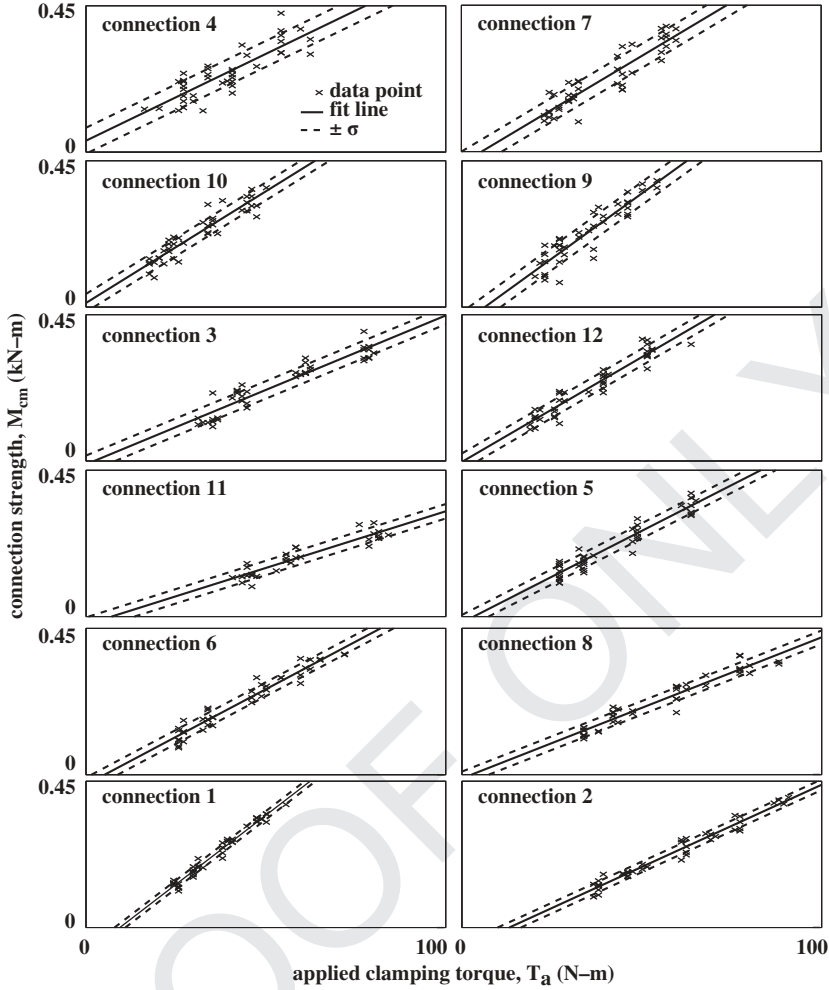


FIGURE 7 Stable M_{cm} vs. T_a calibration data set for each connection.

along the span length. This observation indicates that the nonlinear connections worked as intended with regard to the response of the beam during inter-story drift demands. 255

To generate structures with different fundamental periods, two different superimposed mass configurations were investigated for the six-story frame. Additionally, the lateral strength of the structure was adjusted by prescribing specific moment strengths to the beam-column connections, resulting in four frame configurations (referred to as Frames NL2R2, NL2R4, NL4R2, and NL4R4) with different lateral strengths (representing varying degrees of nonlinearity) as follows. 260

- Frame NL2R2 – two mass plates at each floor and one plate at the roof, with the structure configured to achieve a lateral strength equal to $1/2$ (corresponding to a response modification factor of $R = 2$) of the linear-elastic base shear demand from the median 5%-damped acceleration response spectrum for a suite of 39 unscaled ground motion records described in O'Donnell *et al.* [2012]. 265
- Frame NL2R4 – two mass plates at each floor and one plate at the roof, with the structure configured for a lateral strength equal to $1/4$ ($R = 4$) of the linear-elastic

TABLE 2 Connection variability

| Connection No. | Stand. Dev. σ (kN-M) |
|----------------|-----------------------------|
| 1 | 0.013 |
| 2 | 0.017 |
| 3 | 0.021 |
| 4 | 0.022 |
| 5 | 0.022 |
| 6 | 0.023 |
| 7 | 0.027 |
| 8 | 0.028 |
| 9 | 0.03 |
| 10 | 0.038 |
| 11 | 0.039 |
| 12 | 0.045 |

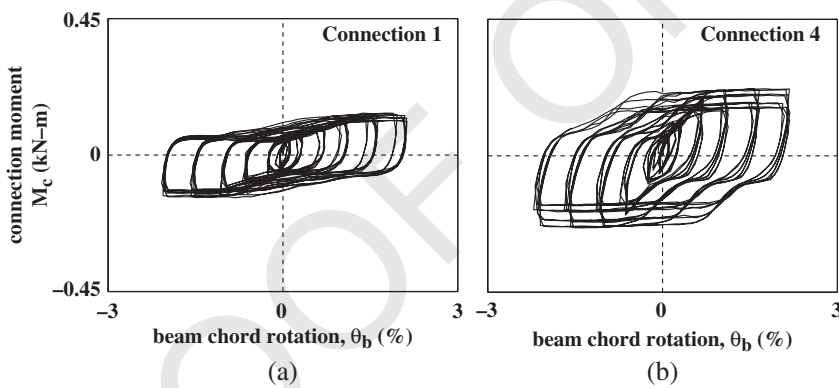


FIGURE 8 Moment-rotation behavior from stable set with applied torque, $T_a = 26$ N-m: (a) Connection 1 (most repeatable) and (b) Connection 4 (least repeatable).

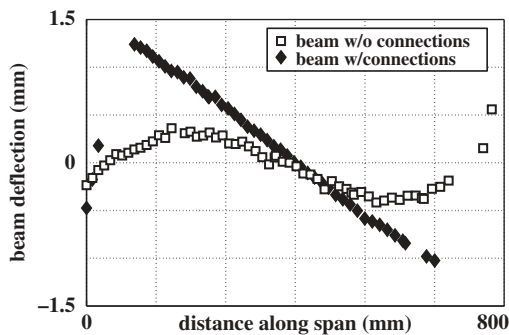


FIGURE 9 Beam deflected shape.

base shear demand from the median 5%-damped response spectrum for the same suite of 39 ground motion records. 270

- Frame NL4R2 – four mass plates at each floor and one plate at the roof, with the structure configured for a lateral strength equal to $1/2$ ($R = 2$) of the linear-elastic demand.
- Frame NL4R4 – four mass plates at each floor and one plate at the roof, with the structure configured for a lateral strength equal to $1/4$ ($R = 4$) of the linear-elastic demand. 275

The beam-column connection moment strengths, M_{cm} to result in the desired lateral strengths for the structures were determined by conducting pseudo-static lateral load tests on the frames. As described in O'Donnell *et al.* [2012], these tests were conducted by holding the fourth floor of the frame stationary while displacing the base laterally using the shake table. The connection layout in Fig. 7 was used and the moment strengths for all 12 connections in each frame configuration were kept constant. 280

Figure 10 shows the hysteretic base shear, V_b vs. 4th floor drift, Δ_4 behavior of the four frame configurations under five repeated reversed-cyclic lateral load tests to observe whether the behavior remained repeatable. Between each test, the shoulder bolt in each connection was loosened, the structure brought back to plumb, and the connection bolts re-tightened to the desired torque based on the regression results in Fig. 7. Since each frame configuration was designed for use under a large number of shake table tests, it was imperative that the structure be reusable and repeatable such that each test started from the same initial conditions with the structure possessing the same properties from test to test. In other words, while the behavior of the structure was allowed to go into the nonlinear range during testing, the initial properties (e.g., lateral stiffness) were required to remain invariant between the tests. The hysteresis plots in Fig. 10 show that the structures exhibited excellent repeatability under static loading. 285 290 295

The linear elastic fundamental period for Frames NL2R2 and NL2R4 was $T_1 = 0.22$ s and for Frames NL4R2 and NL4R4 was $T_1 = 0.27$ s as computed by the transfer function of

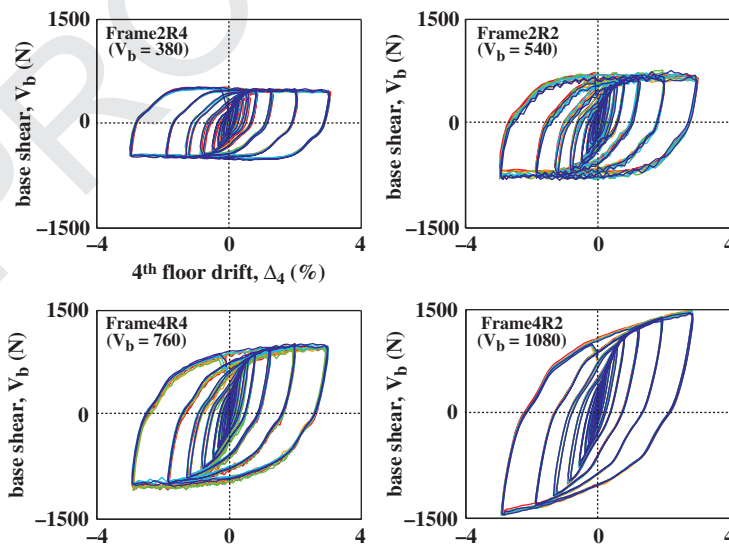


FIGURE 10 Repeated reversed-cyclic V_b - Δ_4 behaviors (five tests for each frame).

the response of the frames to a long duration white noise base excitation. With the selected time-scale of $S_T = 1/3$, the fundamental periods of the test frames correspond to full-scale periods of $T_1 = 0.66$ and $T_1 = 0.82$ s, respectively. Low amplitude white noise excitation rather than resonant sine sweep tests were used to determine the structure periods to ensure that the frames remained in the linear-elastic range during these tests (i.e., rotations of the beam-column connections did not occur).

Following the static lateral load tests and the white noise base excitation tests, each structure was subjected to five repeated dynamic shake table tests under five different input ground motions, resulting in a total of 100 tests for the four frame configurations. The roof drift, Δ_r time history responses from these 100 tests can be seen in Fig. 11 (the different lines in each plot depict the different shake table test trials of the same frame configuration). The corresponding maximum inter-story drift demands, δ_s , over the height of each structure during each dynamic test are provided in Fig. 12.

With a few exceptions, the results in Figs. 11 and 12 generally indicate very good test-to-test consistency in the lateral displacement behaviors of the frames. The five ground motions used in the study, selected from a full suite of 38 records in O'Donnell *et al.* [2012], are listed in Table 3 (note that Record A-CTR270 in the aforementioned reference had to be excluded from the current study). A range of ground motion intensities were selected in order to subject the frames to a broad spectrum of seismic demands. Similar to the static repeatability tests, the dynamic tests were conducted in a non-sequential manner to result in the largest extent of variability possible. Table 4 lists the median, $\hat{\Delta}_r$, and dispersion defined as the coefficient of variation, $\text{COV}(\Delta_r)$, of the peak roof drift demands from each repeated set of five tests, where $\text{COV}(\Delta_r)$ is defined as the standard deviation of the peak roof drift demands divided by the average (i.e., mean) response. The corresponding median, $\hat{\delta}_s$, and coefficient of variation, $\text{COV}(\delta_s)$, of the peak inter-story drift demands (i.e., largest inter-story demand over the height of the structure) are given in Table 5. It can be seen that the $\text{COV}(\Delta_r)$ values for the four frames remained less than 0.05 (or 5%), which is a generally accepted threshold for good repeatability.

However, the results for the peak inter-story drift demands are not as consistent. Two of the ground motions resulted in large (greater than 0.05) $\text{COV}(\delta_s)$ for Frames NL2R2 and NL4R2 (i.e., the two stronger structures). As one would expect, the structures with smaller lateral strength (i.e., Frames NL2R4 and NL4R4) generally experienced larger lateral roof and inter-story drift demands than the structures with larger lateral strength. Frame NL4R4, which had the largest lateral drift demands out of the four frames, also had the largest average variability in the peak roof drift response (i.e., largest average $\text{COV}(\Delta_r)$) and consistently large variability in the peak inter-story drift response (second only to Frame NL2R2).

Given the generally larger variability in the lateral displacements of Frame NL4R4, additional tests were performed on this structure to further investigate and quantify its dynamic response. To investigate this variability, the specimen was subjected to five trials for each of the 38 unscaled ground motion records in O'Donnell *et al.* [2012] resulting in 5 trial responses for each of the 38 input ground motions. As can be seen in Table 5, the dispersion in the peak roof drift demand, $\text{COV}(\Delta_r)$ ranged from a minimum of 1.9% to a maximum of 19.1%. Thus, the structure showed an increased amount of test-to-test variability when subjected to the full suite of 38 records. While this test-to-test variability is above the generally accepted threshold of 5% for good repeatability under a single ground motion record, a more important factor for seismic hazard analysis is the median (i.e., geometric mean) demand from the ground motion suite selected to represent a particular seismic hazard. This median demand is a random variable with uncertainty/variability stemming from the test-to-test variability of the structure response.

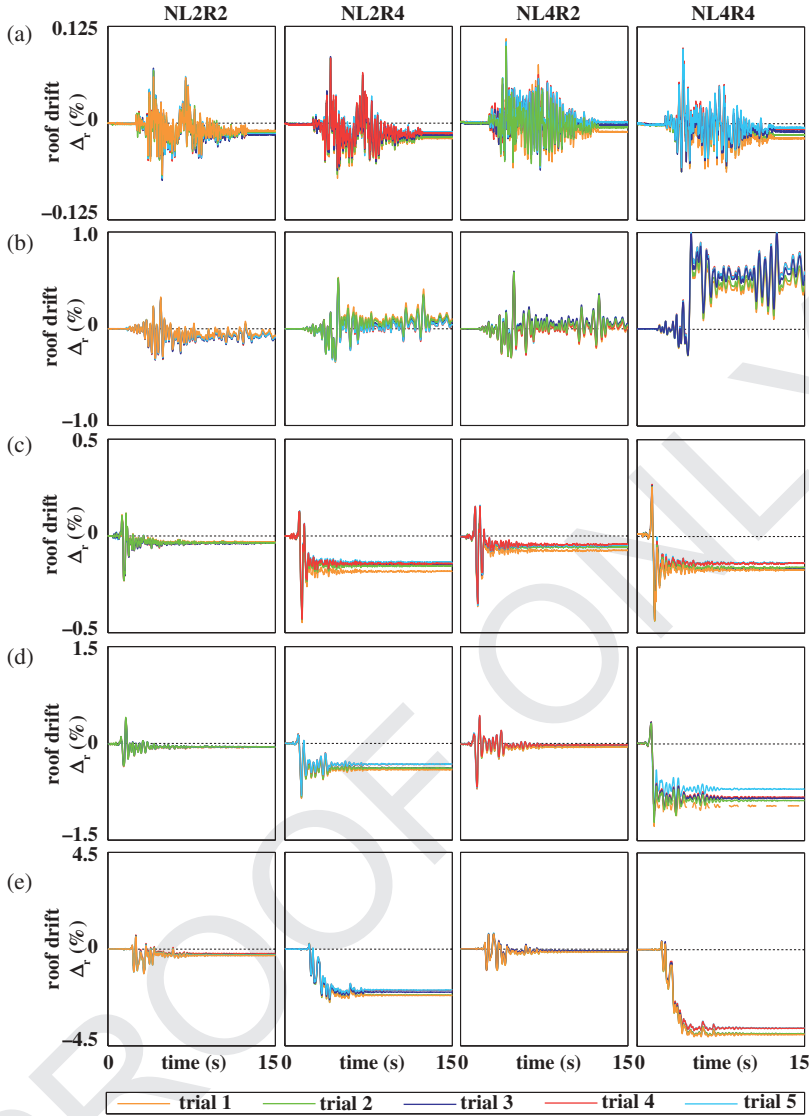


FIGURE 11 Repeatability of dynamic roof drift response, Δ_r for the four frame configurations: (a) 1059-N; (b) FKS090; (c) GIL067; (d) GOF160; and (e) KJM000.

A Monte-Carlo Simulation (MCS) was conducted to investigate this variability to show that the variability in this median demand is less than the acceptable 5% threshold for good repeatability.

The full suite of 38 unscaled ground motions was considered to represent the seismic hazard at a particular site with the median response of the structure to the suite of 38 ground motions assumed to represent the expected seismic demand. For this purpose random combinations of 38 responses from each of the 5 trial shake table tests were generated. A sufficiently large number (500) of such combinations was considered to obtain accurate results based on Monte Carlo statistical analysis; 500 uniformly distributed random sets of 38 integers from 1–5 were generated with each integer for each ground motion determining

350

355

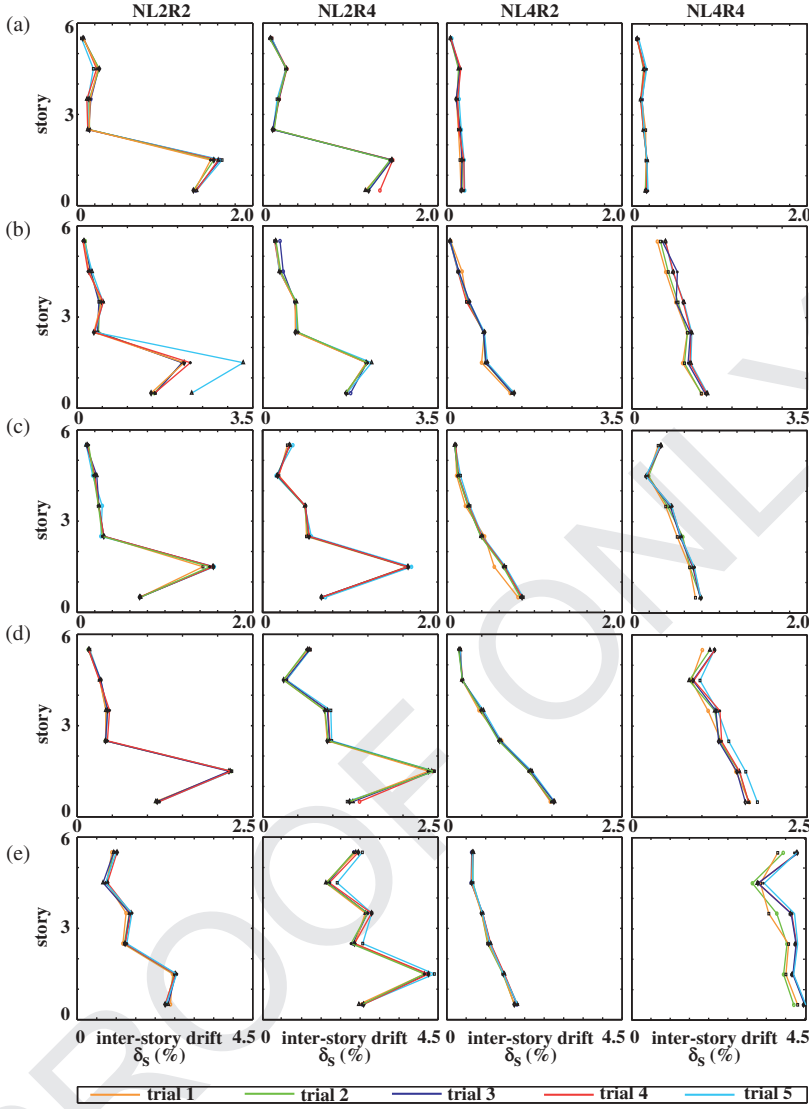


FIGURE 12 Repeatability of maximum inter-story drift ratio, δ_s for the four frame configurations: (a) 1059-N; (b) FKS090; (c) GIL067; (d) GOF160; and (e) KJM000.

the trial test response for that ground motion to be included in the specific combination (i.e., select one Δ_{r1} through Δ_{r5} for each record in Table 6).

The median peak roof drift, $\hat{\Delta}_{r,MCS38}$ over the 38 ground motions was then calculated for each of the 500 combinations and its samples are plotted in Fig. 13a. It can be seen that the median peak roof drift of each of the 500 combinations ranged from a minimum of 0.55% to a maximum of 0.60% indicating a relatively small amount of variability (note that peak roof drifts from the 38 records were much greater than the median values—as large as 6.82% for Frame NL4R4 as shown in Table 6). The corresponding dispersion of the 500 sample medians for the full suite of 38 ground motions, $\text{COV}(\hat{\Delta}_{r,MCS38})$ was calculated as 1.3% by taking the quotient of the standard deviation in the sample medians over

TABLE 3 Selected near-fault ground motion records

| Record ID | Earthquake Name | Station Name | Year | Magnitude M_w | Fault Distance (km) | V_{s30} (m/s) | PGA (g) | MIV (m/s) |
|-----------|-----------------|-----------------------|------|-----------------|---------------------|-----------------|---------|-----------|
| 1059-N | Duzce, Turkey | Lamont 1059 | 1999 | 7.1 | 4.2 | 425 | 0.147 | 0.103 |
| FKS090 | Kobe, Japan | Fukushima | 1995 | 6.9 | 17.9 | 256 | 0.216 | 0.543 |
| GIL067 | Loma Prieta, CA | Gilroy-Gavilan Coll. | 1989 | 6.9 | 10 | 730 | 0.357 | 0.331 |
| GOF160 | Loma Prieta, CA | Gilroy-Historic Bldg. | 1989 | 6.9 | 11 | 339 | 0.284 | 0.777 |
| KJM000 | Kobe, Japan | KJMA | 1995 | 6.9 | 1 | 312 | 0.821 | 1.586 |

TABLE 4 Peak roof drift, Δ_r demand statistics for five trials

| Record ID | Frame NL2R2 | | Frame NL2R4 | | Frame NL4R2 | | Frame NL4R4 | |
|----------------|----------------------|-------------------|----------------------|-------------------|----------------------|-------------------|----------------------|-------------------|
| | $\hat{\Delta}_r$ (%) | COV(Δ_r) | $\hat{\Delta}_r$ (%) | COV(Δ_r) | $\hat{\Delta}_r$ (%) | COV(Δ_r) | $\hat{\Delta}_r$ (%) | COV(Δ_r) |
| 1059-N | 0.071 | 0.047 | 0.085 | 0.012 | 0.102 | 0.036 | 0.093 | 0.048 |
| FKS090 | 0.322 | 0.013 | 0.512 | 0.034 | 0.585 | 0.010 | 0.976 | 0.049 |
| GOL067 | 0.228 | 0.033 | 0.430 | 0.029 | 0.350 | 0.035 | 0.437 | 0.040 |
| GPF160 | 0.399 | 0.025 | 0.827 | 0.029 | 0.680 | 0.020 | 1.210 | 0.043 |
| KJM000 | 1.110 | 0.033 | 2.370 | 0.045 | 0.990 | 0.023 | 3.920 | 0.038 |
| Average | 0.426 | 0.030 | 0.845 | 0.030 | 0.541 | 0.025 | 1.327 | 0.043 |

TABLE 5 Peak inter-story drift, δ_s demand statistics for five trials

| Record ID | Frame NL2R2 | | Frame NL2R4 | | Frame NL4R2 | | Frame NL4R4 | |
|----------------|----------------------|-------------------|----------------------|-------------------|----------------------|-------------------|----------------------|-------------------|
| | $\hat{\delta}_s$ (%) | COV(δ_s) | $\hat{\delta}_s$ (%) | COV(δ_s) | $\hat{\delta}_s$ (%) | COV(δ_s) | $\hat{\delta}_s$ (%) | COV(δ_s) |
| 1059-N | 1.591 | 0.033 | 1.470 | 0.008 | 0.184 | 0.096 | 0.174 | 0.048 |
| FKS090 | 2.339 | 0.221 | 2.097 | 0.021 | 1.310 | 0.023 | 1.449 | 0.039 |
| GOL067 | 1.519 | 0.034 | 1.662 | 0.013 | 0.848 | 0.027 | 0.774 | 0.035 |
| GPF160 | 2.187 | 0.007 | 2.417 | 0.014 | 1.507 | 0.017 | 1.682 | 0.038 |
| KJM000 | 2.505 | 0.016 | 4.235 | 0.025 | 1.780 | 0.023 | 4.394 | 0.029 |
| Average | 2.028 | 0.062 | 2.376 | 0.016 | 1.126 | 0.037 | 1.695 | 0.038 |

the average value of the sample medians. This small variability in the calculated median is important in showing that even though there may be considerable variability for the test-to-test response under particular ground motions as discussed earlier, the variability in the median seismic risk estimate is not large when these excitations are used within an ensemble of ground motions describing the seismic hazard.

To further support this claim, 500 subsets of three distinct ground motions and 500 subsets of seven distinct ground motions were selected from the full suite of 38 records and subjected to a similar MCS procedure as previously described. 500 random combinations of 5 trials were selected for each of the 500 subsets of 7 distinct ground motions and all 125 possible combinations of 5 trials were selected for each of the 500 subsets of 3 distinct ground motions. The specific choice for three and seven ground motion records is motivated by the number of records required in the seismic response history procedures described in ASCE 7 [ASCE, 2010]. The coefficient of variation, COV over the sample median roof drift demands for each ground motion subset was then obtained, quantifying the variability in the seismic demand if this specific smaller subset was used to describe the seismic hazard. Figures 13b and 13c show the distribution of the COVs in the median demands from the 500 subsets of seven and three ground motions, $\text{COV}(\hat{\Delta}_{r,MCS7})$ and $\text{COV}(\hat{\Delta}_{r,MCS3})$, respectively. It can be seen that the expected (i.e., mean) COV is still very low for small ensembles of ground motions, calculated as 3.0% for subsets of seven ground motions and 4.5% for subsets of three ground motions. The largest observed COV in the median roof drift demand was 9.5%, which occurred for a subset of three ground motions.

Since inter-story drift, δ_s is also a parameter of great importance to practitioners performing seismic response history analysis, the same MCS procedure described above was

TABLE 6 Δ_r demands of Frame NL4R4 subjected to 5 trials of 38 ground motions

| Record ID | Δ_{r1} | Δ_{r2} | Δ_{r3} | Δ_{r4} | Δ_{r5} | $\hat{\Delta}_r$ | COV(Δ_r) |
|-----------|---------------|---------------|---------------|---------------|---------------|------------------|-------------------|
| 1058-E | 0.206 | 0.243 | 0.242 | 0.273 | 0.239 | 0.240 | 0.099 |
| 1059-N | 0.093 | 0.098 | 0.087 | 0.090 | 0.097 | 0.093 | 0.048 |
| 1061-E | 0.104 | 0.097 | 0.083 | 0.078 | 0.084 | 0.089 | 0.123 |
| 1062-E | 0.250 | 0.216 | 0.202 | 0.218 | 0.213 | 0.219 | 0.082 |
| 375-N | 0.221 | 0.192 | 0.230 | 0.218 | 0.208 | 0.213 | 0.069 |
| 531-N | 0.079 | 0.091 | 0.074 | 0.075 | 0.085 | 0.081 | 0.088 |
| BOL090 | 0.739 | 0.756 | 0.760 | 0.752 | 0.726 | 0.747 | 0.019 |
| DZC270 | 1.41 | 1.10 | 1.63 | 1.54 | 1.25 | 1.37 | 0.155 |
| AMA090 | 1.38 | 1.28 | 1.77 | 1.37 | 1.33 | 1.41 | 0.138 |
| FKS090 | 0.916 | 0.940 | 1.03 | 1.01 | 0.984 | 0.976 | 0.049 |
| KJM000 | 3.76 | 3.77 | 4.03 | 4.01 | 4.06 | 3.92 | 0.038 |
| NIS090 | 0.400 | 0.661 | 0.552 | 0.585 | 0.643 | 0.560 | 0.183 |
| PRI000 | 5.40 | 4.62 | 4.78 | 4.55 | 4.88 | 4.84 | 0.070 |
| SHI000 | 0.682 | 0.728 | 0.747 | 0.705 | 0.759 | 0.724 | 0.043 |
| TAK090 | 4.24 | 4.59 | 5.10 | 5.44 | 6.82 | 5.17 | 0.191 |
| TAZ090 | 0.965 | 1.05 | 0.990 | 0.945 | 1.01 | 0.990 | 0.040 |
| BRN090 | 0.555 | 0.567 | 0.570 | 0.594 | 0.580 | 0.573 | 0.025 |
| CAP000 | 0.733 | 0.629 | 0.618 | 0.660 | 0.633 | 0.653 | 0.071 |
| CLS000 | 0.760 | 0.828 | 0.851 | 0.843 | 0.841 | 0.824 | 0.045 |
| G02000 | 0.584 | 0.620 | 0.629 | 0.682 | 0.623 | 0.627 | 0.056 |
| G03000 | 0.273 | 0.234 | 0.196 | 0.251 | 0.285 | 0.246 | 0.140 |
| G04000 | 0.605 | 0.579 | 0.530 | 0.481 | 0.598 | 0.557 | 0.094 |
| G06090 | 0.210 | 0.246 | 0.222 | 0.237 | 0.230 | 0.229 | 0.061 |
| GIL067 | 0.441 | 0.407 | 0.442 | 0.449 | 0.448 | 0.437 | 0.040 |
| GOF160 | 1.16 | 1.29 | 1.19 | 1.19 | 1.23 | 1.21 | 0.043 |
| LGP090 | 0.759 | 0.652 | 0.618 | 0.599 | 0.570 | 0.636 | 0.115 |
| LOB000 | 0.197 | 0.215 | 0.191 | 0.198 | 0.202 | 0.201 | 0.045 |
| SJTE225 | 0.243 | 0.252 | 0.238 | 0.222 | 0.220 | 0.235 | 0.060 |
| STG000 | 0.725 | 0.890 | 0.823 | 0.915 | 0.844 | 0.837 | 0.087 |
| UC2090 | 0.182 | 0.149 | 0.174 | 0.172 | 0.156 | 0.166 | 0.083 |
| WAH090 | 0.502 | 0.488 | 0.575 | 0.548 | 0.548 | 0.531 | 0.068 |
| WVC270 | 0.927 | 0.753 | 0.840 | 0.841 | 0.762 | 0.822 | 0.086 |
| CPM000 | 2.33 | 2.69 | 2.93 | 2.84 | 2.83 | 2.72 | 0.088 |
| FOR000 | 0.308 | 0.288 | 0.345 | 0.313 | 0.308 | 0.312 | 0.067 |
| PET090 | 3.34 | 4.39 | 4.76 | 4.38 | 4.78 | 4.30 | 0.135 |
| RIO360 | 0.430 | 0.328 | 0.375 | 0.363 | 0.413 | 0.380 | 0.106 |
| I-ELC180 | 0.336 | 0.363 | 0.384 | 0.380 | 0.383 | 0.369 | 0.055 |
| HEC090 | 0.646 | 0.566 | 0.594 | 0.534 | 0.560 | 0.579 | 0.074 |

applied to the maximum δ_s demands. As shown in Fig. 14, very small degrees of variability were again observed for the dispersion in the median peak (i.e., largest over the height of the structure) inter-story drift demands, with expected (mean) COVs of 3.0% and 4.3% for subsets of seven and three ground motions, respectively. While the peak inter-story drift demand may be representative of the largest extent of strain in a structure during a seismic event, it is not sure whether this demand parameter will exhibit the largest amount

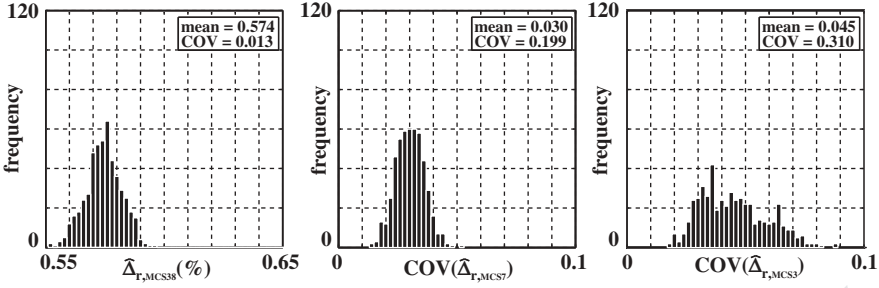


FIGURE 13 Peak roof drift, Δ_r Monte-Carlo Simulation: (a) $\hat{\Delta}_{r,MCS38}$; (b) $\text{COV}(\hat{\Delta}_{r,MCS7})$; and (c) $\text{COV}(\hat{\Delta}_{r,MCS3})$.

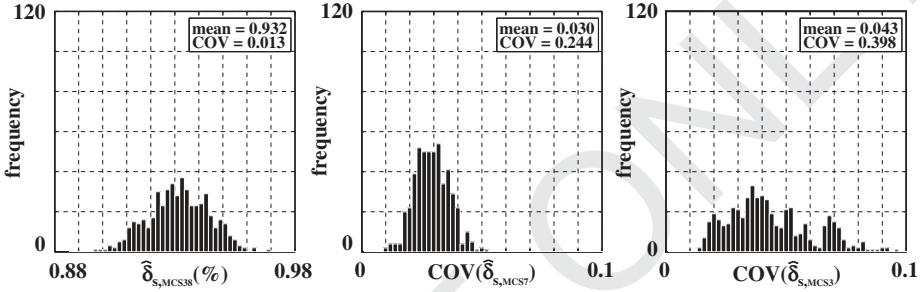


FIGURE 14 Peak inter-story drift, δ_s Monte-Carlo Simulation: (a) $\hat{\delta}_{s,MCS38}$; (b) $\text{COV}(\hat{\delta}_{s,MCS7})$; and (c) $\text{COV}(\hat{\delta}_{s,MCS3})$.

of variability. For this reason, the maximum inter-story drift in each story was also analyzed independently using the same Monte-Carlo subset simulation procedure. The results are presented in Table 7 where it can be seen that the variability in the maximum inter-story drift for each story follows the same trends as the peak roof drift and peak inter-story drift demands. The largest expected (mean) COV was again obtained using subsets of three ground motions and was observed at the 6th story to be 7.5%. Recall that this value is actually lower than the maximum observed dispersion in the peak inter-story drift demand. The reason for this observation is that while the peak inter-story drift can occur at any floor for a given ground motion record, the values for inter-story drifts of each floor are constrained to that particular location in the structure thereby limiting the observed variability in this demand parameter. Furthermore, although this dispersion value is greater than the 5% threshold, it is still quite small given both the small size of the ground motion subset and the comparatively small magnitude of the inter-story drift. Thus, it is concluded that the test structures described in this article can be used in the seismic risk and hazard analysis of nonlinear structures, provided that the median demands from a suite of records are used to quantify the expected demands.

5. Use of Multi-Story Frame Test Structures

While the frame test specimens described in this paper were developed primarily to extend a previous experimental study on ground motion scaling [O'Donnell *et al.*, 2012] to nonlinear structures, there are other potential applications for this research platform. For example,

TABLE 7 Statistics of inter-story drift demands for Frame NL4R4

| Story | $\hat{\delta}_{s,MCS38}$ | | $\text{COV}(\hat{\delta}_{s,MCS7})$ | | $\text{COV}(\hat{\delta}_{s,MCS3})$ | |
|-------|--------------------------|-------|-------------------------------------|-------|-------------------------------------|-------|
| | mean | COV | mean | COV | mean | COV |
| 1 | 0.921 | 0.011 | 0.027 | 0.235 | 0.040 | 0.392 |
| 2 | 0.771 | 0.014 | 0.030 | 0.256 | 0.046 | 0.386 |
| 3 | 0.684 | 0.016 | 0.036 | 0.231 | 0.056 | 0.347 |
| 4 | 0.610 | 0.020 | 0.044 | 0.214 | 0.066 | 0.317 |
| 5 | 0.479 | 0.014 | 0.032 | 0.187 | 0.050 | 0.276 |
| 6 | 0.444 | 0.021 | 0.048 | 0.333 | 0.075 | 0.460 |

the seismic demands from the four frame configurations can be used to evaluate various analytical and design procedures for nonlinear engineering design parameter (EDP) estimation [Krawinkler *et al.*, 2006; ASCE, 2010]. Additionally, the test specimens can be used to investigate damage detection algorithms [Todorovska and Trifunac, 2010] for non-linear structures based on the changes in the building response as the connections go into the nonlinear range representing damage. The connection strength distribution within the frames can be altered to impact the temporal and spatial evolution of damage, thus providing a versatile test bed for comparisons of different damage detection algorithms against measured data of nonlinear seismic structural response. While not possible with the current test frames, it may be possible to develop similar connections for the columns to simulate the development of story mechanisms in the structure as well.

These experimental studies that are envisioned can ultimately be used to validate and support numerical studies, which often rely on a number of modeling assumptions. Some aspects of nonlinear dynamic response are especially difficult to accurately capture using a numerical model. These include the floor accelerations, which are greatly affected by the higher mode vibrations of the structure, and the inter-story residual drifts, which are greatly affected by the permanent plastic offsets in the hinges. Once the structure has reached a full mechanism, its response becomes very sensitive to the amount of plasticization in the hinges. This can be clearly seen in Fig. 11 where the greatest differences between repeated tests occur in the residual drifts upon the full plasticization of the structure. It can also be seen from Fig. 11 that the permanent plastic offsets often governed the peak drifts as well. These effects would be difficult to simulate accurately using a numerical model, where the experimental platform proposed herein can become especially useful.

6. Conclusions

This article describes a novel reusable nonlinear beam-column connection design and an associated frame test structure for the experimental dynamic response history investigation of multi-story buildings subjected to earthquake loading. Calibration tests were performed on the connections as well as four configurations of the test frame to determine their characteristics and variability under static and dynamic loading. The following conclusions can be drawn from the research.

1. Repeated calibration tests showed that the nonlinear beam-column connections initially underwent a period of “stiffening,” but ultimately stabilized to provide a predictable moment-rotation behavior. The resulting calibration data was used to quantify the variability in the connection strength and guide the placement of the

- connections in the test frame, with the connections demonstrating low variability placed lower in the structure to promote more consistent overall frame behavior.
2. Reversed-cyclic lateral load tests of the four frame configurations revealed excellent repeatability under static loading.
 3. The frames showed increased test-to-test variability during dynamic response under some ground motion records from a selected full suite of 38 near-field records. As would be expected, the variability in the inter-story drift demands was higher than the variability in the roof drift demands. 455
 4. While the test-to-test variability in the dynamic response of the structures under some of the earthquakes was large, the variability in the median peak roof drift and inter-story drift demands of the frames from a suite of records was low, even for small subset suites of only three ground motion records. Thus, the test frames described in this article can be used in the seismic risk and hazard analysis of non-linear structures provided that the median demands from a suite of records are used to quantify the expected demands. This conclusion is important in supporting the use of these structures in future investigations on experimental nonlinear dynamic response history testing. Note that the use of median demands is consistent with the seismic response history analysis procedures described in ASCE 7-10, which require the use of average demands when an appropriately selected and scaled suite of seven or more ground motion records is used in design. 460 465 470

Acknowledgments

The authors would like to acknowledge the following individuals: Paulo Bazzurro, University Institute for Superior Studies (IUSS); Sigmund Freeman, Wiss, Janney, Elstner Associates, Inc.; Bob St. Henry, NEFF Engineering; Vladimir Graizer, U.S. Nuclear Regulatory Commission; Farzad Naeim, John A. Martin and Associates, Inc.; and Thomas Sabol, Englekirk & Sabol Consulting Structural Engineers, Inc. The opinions, findings, and conclusions in the article are those of the authors and do not necessarily reflect the views of the organizations or individuals above. 475

Funding

This research is funded by the National Science Foundation (NSF) under Grant No. CMMI 0928662. The support of Dr. K.I. Mehta, current NSF Program Director, and Dr. M.P Singh, former NSF Program Director, is gratefully acknowledged. 480

References

- ASCE [2010]. *Minimum Design Loads for Buildings and Other Structures: ASCE Standard 7-10*, American Society of Civil Engineers. 485
- Dyke, S. J., Spencer Jr., B. F., K., S. M., and D., C. J. [1998] "An experimental study of MR dampers for seismic protection," *Smart Materials and Structures* 7(5). 490
- Elnashai, A. and Di Sarnio, L. [2008] *Fundamentals of Earthquake Engineering*, John Wiley & Sons, West Sussex, UK.
- Erberik, M. A., Sucuoglu, H., and Acun, B. [2012] "Inelastic displacement response of RC systems with cyclic deterioration—An energy approach," *Journal of Earthquake Engineering* 16, 947–962.
- Filiatrault, A., Fischer, D., Folz, B., and Uang, C. [2002] "Seismic testing of two-story woodframe house: Influence of wall finish materials," *Journal of Structural Engineering* 128(10), 1337–1345.

- Goulet, C. A., Haselton, C. B., Mitrani-Reiser, J., Beck, J. L., Deierlein, G., Porter, K. A., and Stewart, J. P. [2007] "Evaluation of the seismic performance of code-conforming reinforced-concrete frame building-From seismic hazard to collapse safety and economic losses," *Earthquake Engineering and Structural Dynamics* **36**(13), 1973–1997. 495
- Grigorian, C., Yang, T., and Popov, E. [1993] "Slotted bolted connection energy dissipaters," *Earthquake Spectra* **9**(3), 491–504. 500
- Ibarra, L. F., Medina, R. A., and Krawinkler, H. [2005] "Hysteretic models that incorporate strength and stiffness deterioration," *Earthquake Engineering & Structural Dynamics* **34**(12), 1489–1511.
- Kim, Y., Kabeyasawa, T., Matsumori, T., and Kabeyasawa, T. [2012] "Numerical study of a full-scale six-story reinforced concrete wall-frame structure tested at E-defense," *Earthquake Engineering & Structural Dynamics* **41**(8), 1217–1239. 505
- Krawinkler, H., Zareian, F., Medina, R. A., and Ibarra, L. F. [2006] "Decision support for conceptual performance-based design," *Earthquake Engineering & Structural Dynamics* **35**(1), 115–133.
- Lafortune, P., McCormick, J., DesRoches, R., and Terriault, P. [2007] "Testing of superelastic recentering pre-strained braces for seismic resistant design," *Journal of Earthquake Engineering* **11**(3), 383–399. 510
- Lignos, D. G., Krawinkler, H., and Whittaker, A. S. [2011] "Collapse assessment of steel moment resisting frames under earthquake shaking," in *Computational Methods in Earthquake Engineering*, Springer, Netherlands. Q4
- McGinnis, M. J., Smith, B., Holloman, M., Lisk, M., O'Donnell, A., and Kurama, Y. C. [2012] "3-D digital image correlation—An underused asset for structural testing," *Structures Congress 2012*, pp. 1958–1969. 515
- Mo, Y. L. and Lee, Y. C. [2000]. "Shake table tests on small-scale low-rise structural walls with various sections," *Magazine of Concrete Research* **52**(3), 177–184.
- Morgen, B. and Kurama, Y. [2008]. "Seismic response evaluation of posttensioned precast concrete frames with friction dampers," *Journal of Structural Engineering* **134**(1), 132–145. 520
- Morgen, B. and Kurama, Y. [2009] "Characterization of two friction interfaces for use in seismic damper applications," *Materials and Structures* **42**(1), 35–49.
- Nader, and Astaneh-Asl. [1996] "Shaking table tests of rigid, semirigid, and flexible steel frames," *Journal of Structural Engineering* **122**(6), 589–596. Q5
- O'Donnell, A. P., Kurama, Y. C., Kalkan, E., Taflanidis, A. A., and Beltsar, O. A. [2012] "Ground motion scaling methods for linear-elastic structures: an integrated experimental and analytical investigation," *Earthquake Engineering & Structural Dynamics* **n/a**(n/a). Q6
- Panagiotou, M., Restrepo, J., and Conte, J. [2011] "Shake-table test of a full-scale 7-story building slice. Phase I: Rectangular wall," *Journal of Structural Engineering* **137**(6), 691–704.
- Rodgers, J. E. and Mahin, S. A. [2003]. "Effects of connection hysteretic degradation on the seismic behavior of steel moment resisting frames," *Pacific Earthquake Engineering Research Center Report PEER-2003/13*, Richmond, California. 530
- Rodriguez, M., Restrepo, J., and Blandón, J. [2007] "Seismic design forces for rigid floor diaphragms in precast concrete building structures," *Journal of Structural Engineering* **133**(11), 1604–1615.
- Schoettler, M. J., Belleri, A., Zhang, D., Restrepo, J. I., and Fleischman, R. B. [2009] "Preliminary results of the shake-table testing for the development of a diaphragm seismic design methodology," *PCI Journal* **54**(1), 25. 535
- Seo, C.-Y. and Sause, R. [2013]. "Nonlinear structural response to low-cut filtered ground acceleration records," *Journal of Earthquake Engineering* **17**, 1212–1232.
- Stavridis, A., Koutromanos, I., and Shing, P. B. [2012] "Shake-table tests of a three-story reinforced concrete frame with masonry infill walls," *Earthquake Engineering & Structural Dynamics* **41**(6), 1089–1108. 540
- Todorovska, M. I. and Trifunac, M. D. [2010] "Earthquake damage detection in the Imperial County Services Building II: Analysis of novelties via wavelets," *Structural Control and Health Monitoring* **17**(8), 895–917. 545
- Way, D. [1996] "Friction-damped moment resisting frames," *Earthquake Spectra* **12**(3), 623–663.